First-principles study of phase equilibria in Cu–Pt–Rh disordered alloys



2009 J. Phys.: Condens. Matter 21 415401

(http://iopscience.iop.org/0953-8984/21/41/415401)

J. Phys.: Condens. Matter **21** (2009) 415401 (7pp) doi:10.1088/0953-8984/21/41/415401

# First-principles study of phase equilibria in Cu–Pt–Rh disordered alloys

**Koretaka Yuge**

Department of Materials Science and Engineering, Kyoto University, Sakyo, Kyoto 606-8501, Japan

Received 3 June 2009, in final form 31 August 2009
Published 23 September 2009
Online at stacks.iop.org/JPhysCM/21/415401

**Abstract**

Phase stability of Cu–Pt–Rh ternary disordered alloys is examined by a combination of cluster expansion techniques and Monte Carlo statistical simulation based on first-principles calculation. The sign of pseudo-binary ECIs indicates that neighboring Cu and Pt strongly prefer unlike-atom pairs, Pt and Rh weakly prefer unlike-atom pairs, and Cu and Rh atoms prefer like-atom pairs, indicating that the ternary alloy retains the ordering tendency of the constituent binary alloys. The formation energy of a random alloy at $T = 1200$ K exhibits a negative sign for a wide range of Pt-rich compositions, while at Pt-poor compositions of $x \leqslant 0.25$, the formation energy has a positive value. Calculated affinities for the random alloy show the variety of energetically favored bonds for the alloy: Cu–Pt bonds in both first- and second-nearest neighbor (1-NN and 2-NN) are energetically preferred for all the composition range, the Pt–Rh bond in 1-NN is preferred at Pt-rich compositions, the Pt–Rh in 2-NN and Rh–Cu in 1-NN bonds are unfavored for all compositions, and the Rh–Cu bond in 2-NN is unfavored for Pt-poor compositions. We elucidate that the ordering tendency of 1-NN and 2-NN Cu–Pt, 2-NN Pt–Rh and 1-NN Cu–Rh atoms in constituent binary alloys is retained for the whole composition range of Cu–Pt–Rh ternary alloys, while that of 1-NN Pt–Rh and 2-NN Cu–Rh atoms significantly depends on composition.

(Some figures in this article are in colour only in the electronic version)

## 1. Introduction

Pt-based alloys have been actively investigated so far in terms of enhancing the high catalytic properties of Pt metal. In particular, the Pt alloy as an anode catalyst in polymer-electrolyte fuel cells (PEFC) is extensively studied in order to depoison CO adsorption for hydrogen-related reactions [1–7]. Since such catalytic properties of the alloys should certainly be controlled by composition and atomic arrangements, the theoretical prediction of structure and phase stability for alloys should be a fundamental and important start to designing desirable Pt-based alloy catalysts in terms of narrowing down the controlling parameters.

Very recently, DFT-based investigations predict that Pt–Rh and Pt–Cu alloys can be potential candidates for the anode catalyst of the PEFC [8, 9]. The alloy surfaces both consist of almost 100% Pt atoms at the surface due to strong Pt segregation to the topmost layer, while the second layer consists mainly of Rh or Cu atoms. The theoretical investigation elucidated that the catalytic property of Pt atoms at the top layer for the alloys is significantly affected by atomic arrangements or composition in the second layer due mainly to the chemical effect between the top and second layers. These facts naturally suggest the possibility of a Cu–Pt–Rh ternary alloy to be a potential candidate for the PEFC catalyst.

Despite such interest, phase stability of the Cu–Pt–Rh alloy in both bulk and surface has not been investigated so far. Meanwhile, phase stability for constituent binary alloys in bulk of Pt–Rh, Pt–Cu and Cu–Rh are investigated both experimentally and theoretically [10–16]: Pt–Cu have a stable ordered structure of $L1_2$ at $Pt_{25}Cu_{75}$ and $L1_0$. Pt–Rh has once been predicted to be a phase-separating system, but recent theoretical [8, 12, 13] as well as experimental [14] work reveals that this alloy exhibits an order–disorder transition below room temperature. Cu–Rh alloy exhibits phase separation and its mixing enthalpy is investigated by experimental study [16].

In the present paper, we investigate phase equilibria of disordered Cu–Pt–Rh alloy using a combination of the cluster expansion [17–19] (CE) technique and first-principles calculation. The effects of a finite temperature on

 

atomic arrangements is considered using Monte Carlo (MC) simulation under a canonical ensemble based on effective cluster interactions (ECIs) obtained via the CE. In the following sections, we discuss the ordering tendency for constituent elemental bonds, formation energies and affinities for the disordered Cu–Pt–Rh alloy.

## 2. Methodology

We summarize the methodology for CE briefly below, since details of the present calculation treatment is published elsewhere [8, 20–22]. The CE technique is adopted to expand DFT energies of Cu–Pt–Rh ternary alloys. In the CE technique, we define the spin variable $\sigma_i = \{+1, 0, -1\}$ which specifies the occupation of Pt, Cu and Rh atoms at lattice point $i$ on the fcc structure. Then we construct cluster functions that are complete and orthonormal for the whole $N$ lattice points [20]:

$$\begin{aligned} E(\vec{\sigma}) &= V_0\Phi_0 + \sum_n \sum_{(\tau)} V_n^{(\tau)}(T)\Phi_n^{(\tau)}(\vec{\sigma}) \\ \Phi_n^{(\tau)} &= \phi_{\tau_1}(\sigma_{n_1})\phi_{\tau_2}(\sigma_{n_2})\cdots\phi_{\tau_n}(\sigma_{n_n}) \\ \phi_0(\sigma_i) &= 1 \qquad \phi_1(\sigma_i) = \sqrt{\tfrac{3}{2}}\sigma_i \\ \phi_2(\sigma_i) &= -\sqrt{2}\left(1 - \tfrac{3}{2}\sigma_i^2\right). \end{aligned} \tag{1}$$

Note that the expansion coefficient $V$, called the effective cluster interaction (ECI), does not depend on atomic arrangements. $\phi(\sigma_i)$ is an orthonormal basis function for lattice point $i$. Two sets of indices should be required to specify the cluster function $\Phi$: one is a set of lattice points $\{i, j, \ldots, k\}$, which configures the cluster figure $n$. Another is a set of indexes of the basis function represented by the subscript of $\phi$, $(\tau)$. While these ECIs have a clear interpretation of coefficients of the orthonormal expansion in equations (1), we do not obtain any intuition of which atomic bonds are energetically preferred or not. Thus we project orthonormal basis functions $\Phi$ onto cluster-probability basis functions, which give an intuitive interpretation in terms of the ordering tendency [23]. Note that, since the cluster-probability basis is not orthonormal, we use them just for seeing the trends of preference for atomic bonds. Using the cluster-probability basis, the contribution of pair clusters to the total energy is given by

$$E_{\text{pair}}(\vec{\sigma}) = -4\sum_{\text{pairs}}^{i}[W_{\text{IJ}}^i\chi_{\text{IJ}}^i + W_{\text{JK}}^i\chi_{\text{JK}}^i + W_{\text{IK}}^i\chi_{\text{IK}}^i], \tag{2}$$

where $\chi_{\text{IJ}}^i$ denotes the probability basis for pair cluster $i$ with I–J atoms and $W_{\text{IJ}}^i$ is the corresponding coefficients, which are called quasibinary effective pair interactions (QEPIs). The QEPI, $W$, can be expressed by a linear combination of the ECIs [20–22] and have an explicit form of

$$W_{\text{IJ}}^i = \tfrac{1}{4}[E_{\text{II}} + E_{\text{JJ}} - E_{\text{IJ}} - E_{\text{JI}}], \tag{3}$$

where $E_{\text{IJ}}$ denotes the average energy of all the atomic arrangements in the Cu–Pt–Rh ternary alloy with I and J atoms in pair cluster $i$. Therefore, $W_{\text{IJ}} > 0$ corresponds to a preference of I–J unlike-atom pairs with respect to I–I and J–J like-atom pairs, and $W_{\text{IJ}} < 0$ to a disfavor of I–J atom pairs.

In order to determine the ECIs, we perform least-squares (LS) fitting of the total energies for Cu–Pt–Rh ordered structures obtained through DFT calculations. We estimate the electronic contribution to the total energy for 174 ordered structures, all consisting of 32 atoms, i.e. a $2 \times 2 \times 2$ expansion of the unit cell in the fcc structure. The first-principles calculations were carried out based on DFT using the Vienna *ab initio* simulation package (VASP) [24–26]. Kohn–Sham equations are solved by employing the projector augmented-wave (PAW) method [27] within the generalized gradient approximation (GGA) of Perdew–Wang91 form [28] to the exchange–correlation functional. A plane-wave cutoff energy of 360 eV is used throughout the calculation. The numerical error was estimated to be of the order of 1 meV/atom by cutoff convergence tests. In order to deal with the possible convergence problems for metals, the Methfessel–Paxton scheme [29] was used with a smearing parameter $\sigma$ of 0.08 eV. Brillouin zone integration is performed on the basis of the Monkhorst–Pack scheme [30] with an $8 \times 8 \times 8$ $k$-point mesh for the 32-atom cell. Geometry optimization including both cell dimensions and atomic coordinates is performed until the residual forces become less than 30 meV $\text{Å}^{-1}$.

For practical application of the cluster expansion, there should be a limitation of the number of DFT input energies as well as the number of clusters that are used for the expansion in equations (1). In the present study, we choose an optimal set of clusters using the genetic algorithm [32, 33] (GA) to minimize the uncertainty of the energies predicted by ECIs, called a cross-validation (CV) score [34, 35]. In the GA, the mutation rate and population size are set to be 0.06 and 30, respectively. An optimal set of input structures are chosen based on the construction of ground-state lines [31]. The details of the above procedures for selecting the clusters and input structures are described in [8, 20].

Combining the CE technique with MC simulation, we can obtain configurational properties for the Cu–Pt–Rh alloys. In order to investigate phase equilibria for Cu–Pt, Pt–Rh, Rh–Cu and Cu–Pt–Rh disordered alloys at finite temperature, the MC statistical thermodynamic simulations under the canonical ensemble are carried out on the Metropolis algorithm. In the MC simulation, temperature $T$ is set at 1200 K, since we confirm that the Cu–Pt–Rh alloy is in a disordered phase over all compositions at $T = 1200$ K. We used an $8 \times 8 \times 8$ expansion of the fcc unit cell (i.e. 2048 atoms) under three-dimensional periodic boundary conditions. At $T = 1200$ K, 10 000 Monte Carlo steps per site were performed for equilibration, followed by 2000 Monte Carlo steps per atom for sampling at each composition. We have confirmed that the MC cell size and steps used are sufficient to achieve equilibrium and to obtain statistically averaged energies: errors of formation energies for Cu–Pt–Rh disordered alloys due to the use of the MC cell size and steps are within about 1–2 meV/atom. In each MC step, the total energy of the system, atomic position and correlation functions were stored. Then the formation energy and affinity for individual atomic

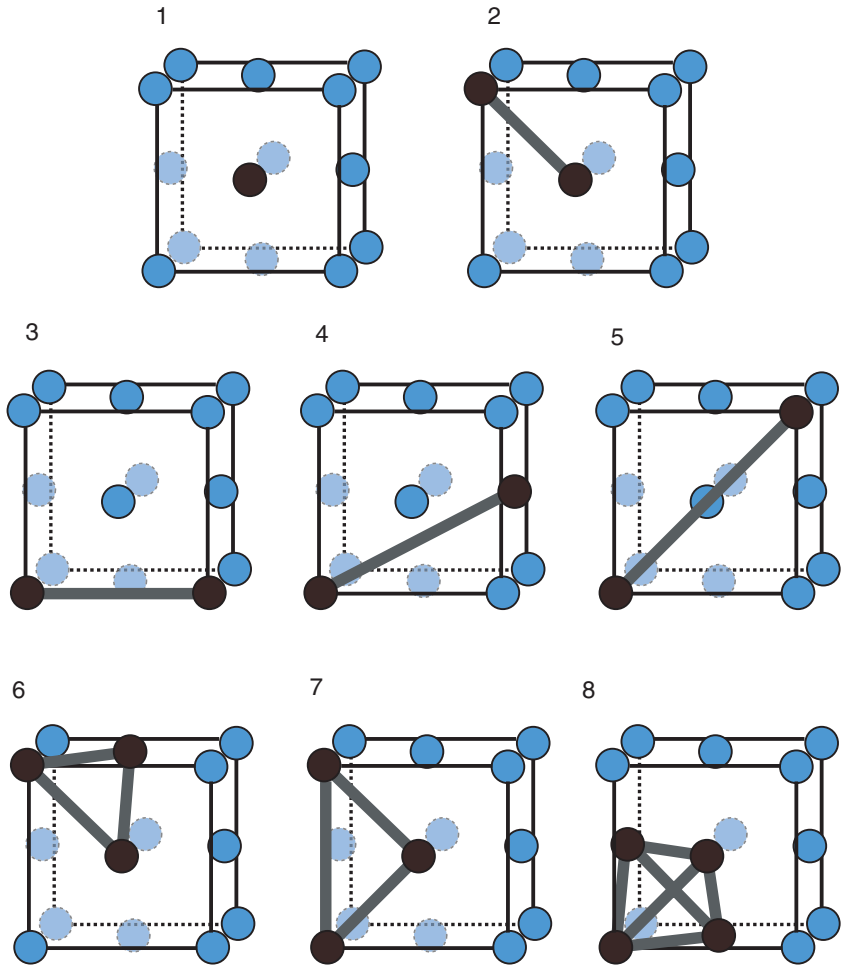


**Figure 1.** Selected multibody clusters in the fcc structure. Note that an empty cluster with no explicit cluster figure is also used in the present CE.

bonds can be obtained by taking the ensemble average. In order to investigate ground-state structures at $T = 0$ K for constituent binary alloys, we perform MC simulation with a simulated annealing algorithm for effectively sweeping across representative formation energies [22]. We employ a 32-atom supercell with seven compositions of $x$ ($0.125 \leqslant x \leqslant 0.875$ with a composition grid of 0.125). Initial temperature of the MC simulation box is at $T = 10\,000$ K and is gradually decreased by 25 K after 6000 Monte Carlo steps per site until the temperature becomes 0 K. During the simulation, all the energies for each MC step are recorded.

## 3. Results and discussion

Following the procedure described in section 2, we determine nine clusters consisting of one empty, one point, four pairs, two triplets and one quadruplet clusters. The multibody cluster figures are shown as dark spheres connected with bold lines in figure 1. These clusters all consist of up to fourth-nearest-neighbor (4-NN) pairs, indicating that total energy for the Cu–Pt–Rh alloy is reasonably characterized by local atomic arrangements. This character was also found for both Pt–Rh and $Pt_{25}Cu_{75}$ binary alloys which require optimal clusters consisting of up to the 4-NN pairs [8, 9]. The set of clusters gives a CV score of 2.1 meV/atom, which is sufficiently accurate to express relative energies for ordered structures. The corresponding ECIs are shown in figure 2, where a set of integers in the parentheses specifies the index of the basis functions in equations (1). It can be clearly seen that the dominant contribution to the total energy comes from ECIs for pair clusters, particularly for 1-NN pair clusters in the basis index set of (1, 1).

In order to see an intuitive interpretation of the ECIs, we estimate the corresponding QEPIs, which are shown in figure 3. There can be seen several important features in the figure: (i) for 1-NN pairs, QEPI for Cu–Pt atoms have the largest positive sign, that for Pt–Rh exhibit a slightly positive value, and that for Cu–Rh shows a large value in negative sign. This certainly reflects the ordering tendency of the constituent binary alloys: the Cu–Pt alloy exhibits a strong ordering tendency, resulting in a stable ordered structure with a high transition temperature of 700–1000 K, depending on composition, the Pt–Rh alloy exhibits a weak ordering tendency with order–disorder transition at an extremely low temperature of around 50–200 K and the Cu–Rh alloy undergoes phase separation. (ii) For Cu–Pt atoms, the QEPI

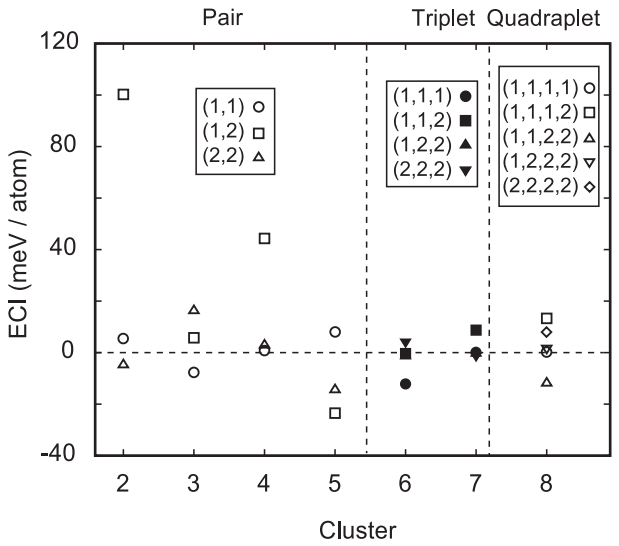


**Figure 2.** Effective cluster interactions for the multibody clusters. A set of integer in the parentheses specifies the index of the basis functions in equations (1).

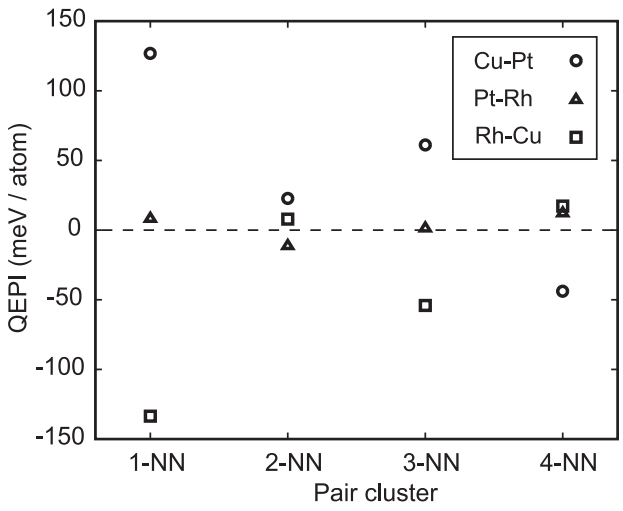


**Figure 3.** Quasibinary effective pair interactions. Open circles denote Cu–Pt pairs; open triangles, Pt–Rh pairs; open squares, Rh–Cu pairs.

for a 2-NN pair is one order smaller than that for 1-NN, which is in contrast to the case of the Cu–Pt binary alloy where ECIs for a 2-NN pair exhibit equal magnitude in positive sign to that for 1-NN [9]. This indicates that the ordering tendency of Cu–Pt atoms along the 2-NN coordination relatively decreases with respect to that along the 1-NN in Cu–Pt–Rh ternary alloy. (iii) For Pt–Rh atoms, QEPIs for 1-NN and 4-NN are in equal magnitude in positive sign and are larger than that for 3-NN, and that for 2-NN exhibits a slightly negative value. This tendency also hold for ECIs for 1- to 4-NN pair clusters in Pt–Rh binary alloys [8]. This indicates that the weak ordering tendency in Pt–Rh binary alloys is certainly retained in the Cu–Pt–Rh ternary alloy. (iv) For Cu–Rh atoms, the dominant contribution to the total energy comes from QEPIs for 1- and 3-NN pairs in negative sign, indicating phase separation in the ternary alloy.

Based on the ECIs in figure 2, we first briefly investigate phase equilibria for constituent Cu–Pt, Pt–Rh and Cu–Rh binary alloys where experimental or theoretical data are available. Figure 4 shows the resultant ground-state diagrams for Cu–Pt, Pt–Rh and Rh–Cu binary alloys. Structures with negative formation enthalpy are represented by small black circles and ground-state structures are represented by large circles. The dotted curves denote simulated mixing enthalpy for disordered alloys at $T = 1200$ K. For the Cu–Pt alloy, three ordered structures are predicted to be the ground state. We successfully find two established ordered structures of $L1_1$ at $Pt_{50}Cu_{50}$ and $L1_2$ at $Pt_{25}Cu_{75}$, which are consistent both with previous theoretical [10] and experimental [11] work. At $Pt_{75}Cu_{25}$, a stable ordered structure has not been experimentally established, but the predicted $L1_2$ structure is consistent with a previous DFT study [10]. Mixing enthalpy for a disordered alloy at equiatomic composition shows 102 meV/atom, which is in good agreement with the measured enthalpy of ∼114 meV/atom at $T = 1350$ K [11]. For the Pt–Rh alloy, we predict four ordered structures in the ground state: '40' at $Pt_{50}Rh_{50}$ and $D0_{22}$ at $Pt_{25}Rh_{75}$ are consistent with both early DFT-based theoretical [12, 13] and experimental [14] studies. $D0_{22}$ at $Pt_{75}Rh_{25}$ is not consistent with the early theoretical [12] study, but agrees with a more recent DFT-based theoretical prediction [13]. Note that predicted ordered structures are all superlattices along the [210] direction (i.e. alternate stacking of Pt and Rh atoms along the [210] direction with the number of stacking layers depending on composition), which also holds for the ordered structures previously predicted by DFT calculations [12, 13]. This ordering tendency is also confirmed by a diffuse x-ray scattering study [14], where the short-range order parameter shows its maximum at the W point of [1 1/2 0] in the reciprocal space. Therefore, we can successfully predict the characteristic ordering tendency along the [210] direction for the Pt–Rh alloy. For Rh–Cu, as predicted by the signs of QEPIs in figure 3, there is found to be no stable ordered structure. Mixing enthalpy $\Delta H$ for Pt–Rh and Cu–Rh alloys has been experimentally investigated based on a pseudosubregular model. At equiatomic composition, we estimate $\Delta H$ to be $-16$ and $+82$ meV/atom for Pt–Rh and Cu–Rh alloys, which are both in qualitative agreement with $\sim -28$ and $\sim +120$ meV/atom at $T = 1273$ and 1275 K from the previous measurement [15, 16]. The difference between the measured and the present theoretical value could be partially due to the use of a pseudosubregular model for excess entropy in the measurement, which assumes an entropy expression of the same type of functional dependence of composition for mixing enthalpy. To summarize, we successfully predict energetics of both ground-state ordered structures and disordered state for the constituent binary alloys within established theoretical and experimental data.

We now proceed with our discussion about energetics of the disordered state to the Cu–Pt–Rh ternary alloy. Figure 5 shows a ternary diagram of formation energy for the Cu–Pt–Rh disordered alloy at $T = 1200$ K. It can be seen that the topology of the formation energy landscape seems similar to

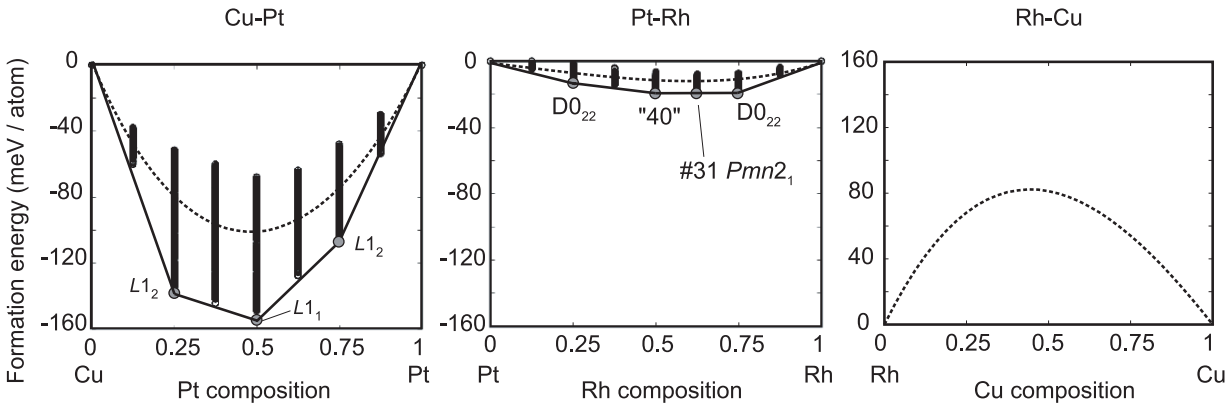


**Figure 4.** Ground-state diagram for Cu–Pt, Pt–Rh and Rh–Cu binary alloys obtained via MC simulations. Structures with negative formation enthalpy are represented by small black circles and ground-state structures are represented by large circles with its structure name. The dotted curves denote mixing enthalpy for disordered alloys at $T = 1200$ K.

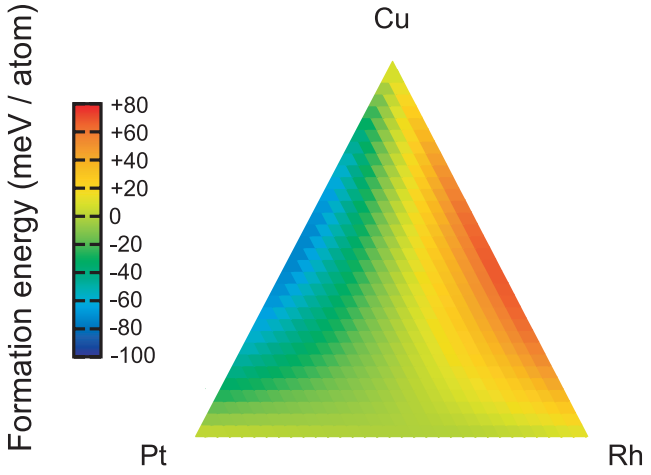


**Figure 5.** Ternary diagram of formation energy for Cu–Pt–Rh disordered alloy at $T = 1200$ K.

constituent binaries: the upper and lower limits of formation energy for the ternary alloy correspond to the lowest and highest formation energy for Cu–Pt and Cu–Rh binary alloys, respectively. Formation energy of constituent binaries of Cu–Pt, Pt–Rh and Cu–Rh gradually get close to zero when the composition of the other elements increases. As a result, there can be seen a wide range of compositions for a significantly weak mixing tendency of $-20 \leqslant \Delta E_{\text{form}} \leqslant 20$ meV/atom, which is illustrated by the yellow and greenish yellow areas in figure 5.

At finite temperature, the disordered alloy should have a weak ordering or clustering tendency due to the competition between configuration entropy and mixing energy. In order to see which atomic bonds are likely to be ordering or clustering in the ternary alloy, we introduce the affinity $\alpha$, which is defined as

$$\alpha_n^{\text{IJ}} = \frac{y^{\text{IJ}}(\text{system})}{y^{\text{IJ}}(\text{random})} - 1, \tag{4}$$

where $y^{\text{IJ}}(\text{system})$ and $y^{\text{IJ}}(\text{random})$ represent the pair probability of I–J elements for the system and completely disordered alloy, respectively. Therefore, $\alpha^{\text{IJ}} > 0$ represents a preference of I–J bonds and $\alpha^{\text{IJ}} < 0$ disfavor. For a completely random alloy, the pair probability of the I–J pair, $y^{\text{IJ}}(\text{random})$, is simply given by $2c_{\text{I}}c_{\text{J}}$, where $c_{\text{I}}$ and $c_{\text{J}}$ denote composition of I and J elements, respectively. Figure 6 shows the ternary diagram of the resultant simulated affinity along the 1-NN and 2-NN coordination for the Cu–Pt–Rh ternary disordered alloy. Cu–Pt atoms along the 1-NN and 2-NN coordination both exhibit large values in positive sign for almost all the composition range, indicating a strong ordering tendency along these coordinations for the whole composition. This tendency should reflect positive values in QEPIs for the 1-NN and 2-NN Cu–Pt pairs shown in figure 3. For Pt–Rh atoms, the ordering tendency significantly depends on both composition and coordination: at a Pt-rich composition, Pt–Rh atoms in the 1-NN are preferred while at a Pt-poor composition, disfavor of the Pt–Rh atoms can be seen. Since the 1-NN Pt–Rh pair is energetically preferred in the Pt–Rh binary alloy [8], the ordering tendency for the 1-NN pair in the binary alloy is retained in the Pt-rich composition, which is disrupted when the composition of Pt decreases. The affinity for 2-NN Pt–Rh atoms exhibits a negative sign for the whole composition range. Since the 2-NN Pt–Rh pair is energetically disfavored in the Pt–Rh binary alloy [8], the ordering tendency for the 2-NN pair in the binary Pt–Rh alloy is retained for the whole ternary composition range. The affinity for 1-NN Cu–Rh atoms exhibits a negative sign for almost all the composition range except for significant Cu-rich composition. Since the Cu–Rh binary alloy undergoes phase separation due mainly to the significant disfavor of 1-NN Cu–Rh atoms, this tendency in the binary alloy is retained for the ternary alloy, which certainly reflects the large value in negative sign of QEPI for 1-NN Cu–Rh, as shown in figure 3. 2-NN Cu–Rh atoms are disfavored at Pt-poor compositions, while it is preferred at Pt-rich compositions. To summarize, the ordering tendency of 1-NN and 2-NN Cu–Pt, 2-NN Pt–Rh and 1-NN Cu–Rh atoms in constituent binary alloys is retained for the whole composition range of Cu–Pt–Rh ternary alloys, while that of 1-NN Pt–Rh and 2-NN Cu–Rh atoms significantly depends on the composition.

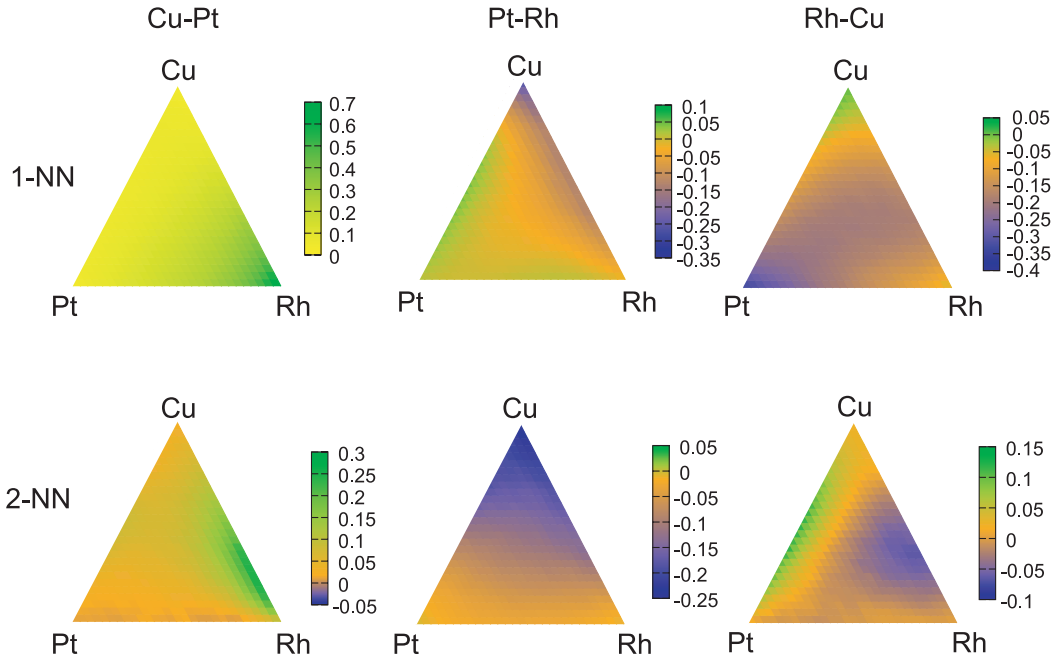


**Figure 6.** Calculated affinity $\alpha$ along the 1-NN and 2-NN coordination for Cu–Pt–Rh ternary disordered alloy at $T = 1200$ K.

## 4. Conclusions

Phase stability of Cu–Pt–Rh ternary disordered alloys is investigated by a combination of cluster expansion techniques and Monte Carlo statistical simulation based on first-principles calculation. First, we have successfully predicted the energetics for both ordered and disordered constituent binary Cu–Pt, Pt–Rh and Rh–Cu alloys by comparing previous experimental as well as theoretical investigations. Quasibinary effective pair interactions indicate that neighboring Cu and Pt strongly prefer unlike-atom pairs, Pt and Rh weakly prefer unlike-atom pairs, and Cu and Rh atoms prefer like-atom pairs. This indicates that the ordering tendency in constituent binary alloys is retained in the ternary Cu–Pt–Rh alloy. Formation energy of a random alloy at $T = 1200$ K below the melting temperature exhibits a negative sign for a wide range of Pt-rich compositions, while at Pt-poor compositions of $x \leqslant 0.25$, the formation energy has a positive value. The upper and lower values of formation energy correspond to the maximum and minimum formation energy for Cu–Rh and Cu–Pt binary alloys, respectively. We investigate weak ordering or clustering tendency for the disordered alloy based on affinities: Cu–Pt bonds in both first-and second-nearest neighbor (1-NN and 2-NN) are energetically preferred for all the composition range, the Pt–Rh bond in 1-NN is preferred at Pt-rich compositions, the Pt–Rh in 2-NN and Rh–Cu in 1-NN is unfavored for all compositions and the Rh–Cu bond in 2-NN is unfavored for Pt-poor compositions. We elucidate that the ordering tendency of 1-NN and 2-NN Cu–Pt, 2-NN Pt–Rh and 1-NN Cu–Rh atoms in constituent binary alloys is retained for the whole composition range of Cu–Pt–Rh ternary alloys, while that of 1-NN Pt–Rh and 2-NN Cu–Rh atoms significantly depends on the composition.

## Acknowledgment

This research was supported by a Grant-in-Aid for Young Scientists Start-up (20860048) from the Japan Society for the Promotion of Science (JSPS).

## References

[1] Stamenkovic V, Mun B S, Mayrhofer K J J, Ross P N, Markovic N M, Rossmeisl J, Greeley J and Norskov J K 2006 *Angew. Chem.* **118** 2963
[2] Christoffersen E, Liu P, Ruban A, Skriver H K and Norskov J K 2001 *J. Catal.* **199** 123
[3] Ruban A, Hammer B, Stoltze P, Skriver H L and Norskov J K 1997 *J. Mol. Catal.* A **115** 421
[4] Pallassana V, Neurock M, Hansen L B and Norskov J K 2000 *J. Chem. Phys.* **112** 5435
[5] Hirschl R, Delbecq F, Sautet P and Hafner J 2002 *Phys. Rev.* B **66** 155438
[6] Tang H and Trout B L 2005 *J. Phys. Chem.* B **109** 17630
[7] Tang H and Trout B L 2005 *J. Phys. Chem.* B **109** 6948
[8] Yuge K, Seko A, Kuwabara A, Oba F and Tanaka I 2006 *Phys. Rev.* B **74** 174202
[9] Yuge K, Seko A, Kuwabara A, Oba F and Tanaka I 2007 *Phys. Rev.* B **76** 045407
[10] Lu Z W, Wei S-H, Zunger A, Frota-Pessoa S and Ferreira L G 1991 *Phys. Rev.* B **44** 512
[11] Hultgren R, Desai P D, Hawkins D T, Gleiser M and Kelley K K 1973 *Selected Values of the Thermodynamics Properties of Binary Alloys* (Metals Park, OH: American Society for Metals)
[12] Lu Z W, Klein B M and Zunger A 1995 *J. Phase Equilib.* **16** 36
[13] Curtarolo S, Morgan D and Ceder G 2005 *CALPHAD: Comput. Coupling Phase Diagr. Thermochem.* **29** 163
[14] Steiner Ch, Schönfeld B, Portmann M J, Kompatscher M, Kostorz G, Mazuelas A, Metzger T, Kohlbrecher J and Deme B 2005 *Phys. Rev.* B **71** 104204
[15] Jacob K T, Priya S and Waseda Y 1998 *Metall. Mater. Trans.* A **29A** 1545

[16] Priya S and Jacob K T 2000 *J. Phase Equilib.* **21** 342
[17] Sanchez J M, Ducastelle F and Gratias D 1984 *Physica* A **128** 334
[18] de Fontaine D 1994 *Solid State Physics* vol 47, ed H Ehrenreich and D Turnbull (New York: Academic) pp 33–176
[19] Clouet E, Sanchez J M and Sigli C 2002 *Phys. Rev.* B **65** 094105
[20] Yuge K, Seko A, Koyama Y, Oba F and Tanaka I 2008 *Phys. Rev.* B **77** 094121
[21] Yuge K 2009 *J. Phys.: Condens. Matter* **21** 055403
[22] Yuge K 2009 *Phys. Rev.* B **79** 144109
[23] Wolverton C and de Fontaine D 1994 *Phys. Rev.* B **49** 8627
[24] Kresse G and Hafner J 1993 *Phys. Rev.* B **47** R558
[25] Kresse G and Furthmüller J 1996 *Phys. Rev.* B **54** 11169
[26] Kresse G and Joubert D 1999 *Phys. Rev.* B **59** 1758
[27] Blöchl P E 1994 *Phys. Rev.* B **50** 17953
[28] Perdew J P and Wang Y 1992 *Phys. Rev.* B **46** 6671
[29] Methfessel M and Paxton A T 1989 *Phys. Rev.* B **40** 3616
[30] Monkhorst H J and Pack J D 1976 *Phys. Rev.* B **13** 5188
[31] Blum V and Zunger A 2004 *Phys. Rev.* B **70** 155108
[32] Hart G L W, Blum V, Walorski M J and Zunger A 2005 *Nat. Mater.* **4** 391
[33] van de Walle A 2005 *Nat. Mater.* **4** 362
[34] Stone M 1974 *J. R. Stat. Soc.* B **36** 111
[35] Allen D M 1974 *Technometrics* **16** 125